Direct Electrochemical Determination of Thermodynamic Factors in Aprotic Binary Electrolytes

Johannes Landesfeind,[a,=,z] Andreas Ehrl,[b,=,z] Maximilian Graf,[a] Wolfgang A. Wall,[b] and Hubert A. Gasteiger[a,*]

[a]*Chair of Technical Electrochemistry, Department of Chemistry and Catalysis Research Center, Technische Universität München, Munich, Germany*
[b]*Institute for Computational Mechanics, Department of Mechanical Engineering, Technische Universität München, Munich, Germany*

We propose a novel method to determine the thermodynamic factor of binary salts dissolved in aprotic solvents as a function of salt concentration. The method is based on cyclic voltammetry experiments conducted in a three-electrode cell with the ferrocene/ferrocenium redox couple being used as an internal standard. The main advantage of this experimental setup is the direct electrochemical determination of the thermodynamic factor from a single type of experiment without the necessity of additional assumptions on other transport parameters. The theoretical derivation of the used relationship between peak/half-wave potentials and the thermodynamic factor as well as non-ideal effects which distort the experimental results, such as uncompensated resistances or concentration overpotentials are discussed in detail. Different strategies are suggested to avoid these non-ideal effects using the peak separation of the cyclic voltammograms as an inherent quality measure for the experimental data. Applicability of the experimental procedure is demonstrated for $LiClO_4$ in EC:DEC (1:1, w:w) in the range from 5 mM to 2 M and repeated for typical $LiPF_6$ containing electrolytes. At the end, the obtained results are compared to thermodynamic factors of similar electrolyte solutions published in literature.

 [DOI: 10.1149/2.0651607jes]

Manuscript submitted January 18, 2016; revised manuscript received April 4, 2016. Published April 19, 2016.

Advanced numerical simulation tools are important both for understanding existing battery systems such as lithium-ion batteries and for the development of future battery systems as, e.g., lithium-sulfur batteries. One beneficial aspect of computational methods is that they can provide insight into physical and chemical aspects, which sometimes cannot be probed by experimental methods. For such numerical simulations, accuracy and reliability are key issues and depend on appropriate physical models, boundary conditions, and accurately determined physico-chemical parameters. Standard ion-transport models for concentrated binary electrolyte solutions depend on three ion transport parameters, namely the conductivity, the transference number and the binary diffusion coefficient.[1,2] In addition to the transport parameters, the thermodynamic factor $(1 + \mathrm{d}\ln f_{\pm}/\mathrm{d}\ln c)$ which is derived from the mean molar activity coefficient $f_{\pm}$ is required for the correct description of the thermodynamic behavior of a binary electrolyte solution. In general, the focus in the literature is on the determination of ion transport parameters, while only few publications deal with the determination of mean molar activity coefficients or thermodynamic factors, especially in the case of non-aqueous electrolytes.

Some publications on activity coefficients and thermodynamic factors in non-aqueous electrolytes are summarized shortly in the following. In Bartel et al.,[3] the osmotic coefficient is determined based on the vapor pressure of lithium perchlorate ($LiClO_4$) in various alcohols. The data for the osmotic coefficients are well represented by the Pitzer equation with seven parameters. Two of the necessary parameters are assumed based on literature values, whereas the remaining parameters are determined by a regression model. In that publication, the mean molal (i.e., based on $mol/kg_{solvent}$) activity coefficient $\gamma_{\pm}$ rather than the mean molar activity coefficient $f_{\pm}$ (i.e., based on $mol/l_{electrolyte}$) is calculated from the osmotic coefficient by integration. Later on, the authors use the same approach for aprotic electrolyte solutions such as $LiClO_4$ dissolved in dimethylcarbonate (DMC).[4] In Stewart and Newman, the osmotic coefficient for lithium hexaflurophosphate ($LiPF_6$) in ethylene carbonate (EC) is determined by melting point depression.[5] However, this method may not be applicable to all solvent mixtures and the complete concentrations range since, according to the authors, it is limited by the eutectic point of the solvent mixture. In the same publication, the mean molar activity coefficient of $LiPF_6$ in EC:EMC (1:1, w:w) is also determined based on experiments in a concentration cell, whereby a constant, i.e., concentration-independent transference number was assumed. In Valøen et al., this approach is also used for $LiPF_6$ in PC:EC:EMC (10:27:63, v:v:v).[6] In addition, the temperature dependence of the mean molar activity coefficient is determined in the range from 263 K–333 K. The validity of a constant transference number is verified by experiments using the Hittorf method and data available in the literature. However, a theoretical explanation for the assumption of a constant transference number is missing in both contributions. In Nyman et al., the diffusion coefficient, transference number, and thermodynamic factor are determined for $LiPF_6$ in EC:EMC (3:7, w:w) by a numerical optimization approach, based on relaxation experiments in a polarization cell with a porous separator in combination with data from a concentration cell.[7] The numerical optimization algorithm is based on concentrated solution theory, incorporating the solvent velocity into the mass balance. Recently, the temperature dependence of $LiPF_6$ dissolved in EC:DEC (1:1, w:w) was investigated by the same method.[8] Binary diffusion coefficient, transference number, and thermodynamic factor can also be determined through a combination of three experimental setups. In this approach, the diffusion coefficient is measured by a galvanostatic relaxation experiment as presented, e.g., in Harned and French.[9] The concentration cell and a galvanostatic polarization experiment are then used to calculate the remaining two parameters.[10]

The basic objective of the present contribution is the *electrochemical* determination of the thermodynamic factor for aprotic binary electrolyte solutions within a *single* experimental setup. Therefore, cyclic voltammetry in electrolyte solutions containing small amounts of ferrocene are measured versus a lithium reference electrode, showing that the peak positions of the ferrocene redox couple can be related to the mean molar activity coefficient of the lithium salt. The use of the ferrocene redox couple as a quasi-reference is discussed in detail in the original contribution by Gritzner and Kuta.[11] In this context, the lithium salt is referred to as supporting electrolyte, since the ferrocene concentration is kept at least an order of magnitude lower concentration than the lithium salt. In the Experimental section, setup

[=]These authors contributed equally to this work.
*Electrochemical Society Fellow.
[z]E-mail: j.landesfeind@tum.de; ehrl-andreas@tum.de

Figure 1. Three-electrode glass setup with a Pt CE (left) and a Au WE (center) in EC:DEC (1:1 w:w) electrolyte containing $LiClO_4$ concentrations from 0.1×10^{-3} to 2 M and 50 μM Fc (ferrocene) as well as a metallic Li RE (right) in the same electrolyte without Fc.

and procedure are described in detail. The basic relation between the peak position and the mean molar activity coefficient is derived thereafter, and theoretical factors distorting experimental results are reviewed. Subsequently, experimental results are presented and experimental strategies are discussed which minimize errors caused by experimental constraint. Experimental data are selected depending on their peak separation and used to determine the parameters of an extended Debye-Hückel law. Obtained activity coefficients are then used to calculate the thermodynamic factor. By applying this procedure at various temperatures using a slightly modified cell design, meaningful values for the concentration dependent thermodynamic factor can be obtained.[12] Finally, the concentration dependent thermodynamic factors are compared to data available in the literature.

Experimental

Measurements and electrolyte preparations were performed in an argon filled and temperature controlled glove box (from MBraun, with temperature at 25°C ± 1°C, water content <0.1 ppm, and Ar 5.0 (Westfalen)). A custom made three-electrode glass setup (Figure 1) was used with a platinum (Advent, 99.99+% purity) counter electrode (CE), gold (Alfa Aesar, 99.999% purity) working electrode (WE), and a lithium (Rockwood Lithium, 0.45 mm, high purity) reference electrode (RE). Individual cell compartments were separated by porous glass frits. The distance between the electrodes was kept small (∼1 cm) to minimize ohmic drops in the electrolyte phase. To prevent electrolyte evaporation, the cell is sealed with PTFE sealing rings (Glindemann) at the glass joints and the electrodes are electronically connected with the potentiostat via fused-in tungsten wires. All glass cell parts were cleaned by boiling them in a mixture of ethanol and water (Millipore, Elix, 15 MΩ cm), thoroughly rinsed with water, and then dried at 70°C in a heating oven before bringing them into the glove box. Relative solvent permittivities were measured in a custom made coaxial stainless steel setup using impedance spectroscopy.

A mixture of ethylene carbonate (EC, 50 w%, Sigma Aldrich, anhydrous, 99%) and diethyl carbonate (DEC, 50 w%, Sigma Aldrich, anhydrous, >99%) was used as solvent for the investigated electrolytes with $LiClO_4$ (Sigma Aldrich, 99.99%) concentrations from 0.1×10^{-3} to 2 M. Ferrocene (Fc, Merck, >98%) was added to the electrolyte in the CE and WE compartment at equal concentrations of 50 μM or 100 μM. As usual, due to the small association constant of comparable electrolytes, 48 dm^3/mol for LiClO4 in PC/EMC,[13] ion pair formation is neglected in this work.[3–10] In consecutive measurement series with multiple $LiClO_4$ concentrations, smallest concentrations were measured first to avoid contaminations by salt remains from previous experiments. For repetitive measurements on different electrolytes, $LiPF_6$ (Sigma Aldrich, 99.99%), EMC (Sigma Aldrich, 99.99%) and DMC (Sigma Aldrich, >99.99%) were used for electrolyte preparations.

A Biologic VMP3 potentiostat/galvanostat was connected to the cell placed inside the glove box using actively shielded cables. The cell impedance was measured and the high frequency resistance between WE and RE was extracted by linear extrapolation of the high frequency part in a Nyquist plot. Recorded cyclic voltammograms (CVs) between 2.5 V and 4 V versus Li/Li^+ were online IR-corrected for different percentages of the determined WE-RE resistance, usually 85%. Always five consecutive scans were performed per analyzed scan rate (10 mV/s or 20 mV/s).

Theory

In this section, a general correlation between the cell potential U and the mean molar activity coefficient $f_\pm(c)$ of a binary salt is derived for cyclic voltammetry experiments. The used experimental setup is shown in Figure 1 and the meaning and units of each symbol are given in the List of Symbols/Constants at the end of this article. The cell potential U is the difference between the electrostatic potential of the Working Electrode (WE) Φ_{WE} and the electrostatic potential of the lithium Reference Electrode (RE) Φ_{RE}. The concentration dependence of the mean molar activity coefficient is expressed in terms of the concentration of a binary salt, which is defined as $c = c_+/\nu_+ = c_-/\nu_-$. Here, c_+ and c_- denote the molar concentration of the positive and negative ionic species, respectively. The coefficients ν_+ and ν_- describe the stoichiometry of the salt decomposition into its ionic components. In general, the mean binary activity coefficient of any salt is defined as

$$f_\pm^\nu \equiv f_+^{\nu_+} f_-^{\nu_-} \quad [1]$$

where ν is given by $\nu = \nu_+ + \nu_-$. Subsequently, the subscripts '+' and '−', indicating the positive and negative ionic species, are replaced by the names of their corresponding ions, namely lithium $Li^+$and perchlorate ClO_4^- for clarity. Generally the described framework can also be applied to any other binary salt. As mentioned before, the lithium perchlorate salt can also be thought of as a supporting electrolyte, whereas ferrocene (Fc) or its oxidized form ferrocenium (Fc^+) are the minor ionic species in the electrolyte solution.

Theoretical derivation.—The redox reaction at the Reference Electrode (RE) is defined as

$$Li \rightleftarrows Li^+ + e^- \quad [2]$$

and at the Working Electrode (WE) as

$$Fc \rightleftarrows Fc^+ + e^- \quad [3]$$

where Fc denotes the ferrocene and Fc^+ the ferrocenium ion. The reaction Gibbs energy $\Delta_R G$ for the lithium reaction at the RE is given by

$$\Delta_R G|_{RE} = 0 = \mu_{Li} - \tilde{\mu}_{Li^+} - \tilde{\mu}_{e^-} \quad [4]$$

and for the ferrocene reaction at the WE by

$$\Delta_R G|_{WE} = \mu_{Fc} - \tilde{\mu}_{Fc^+} - \tilde{\mu}_{e^-}. \quad [5]$$

Here, μ denotes the chemical potential of an uncharged component and $\tilde{\mu}$ the electrochemical potential of an ionic species. The reaction Gibbs energy of the RE is zero, since the reference electrode is always in an equilibrium state due to negligible current flow across its interface. As a result, the cell potential U expressed in terms of the electrochemical potentials of the electrons e^- in WE and RE

$$FU = F(\Phi_{WE} - \Phi_{RE}) = \tilde{\mu}_{e^-}|_{RE} - \tilde{\mu}_{e^-}|_{WE} \quad [6]$$

can be written as

$$FU = (\mu_{Li} - \tilde{\mu}_{Li^+})|_{RE} - (\mu_{Fc} - \tilde{\mu}_{Fc^+} - \Delta_R G)|_{WE}, \quad [7]$$

where the cell potential is determined by the reactions at the interfaces of WE and RE. The electrochemical potential of an arbitrary ionic species k for any electrolyte can be defined, according to Newman and Thomas-Aleya, as

$$\tilde{\mu}_k = z_k \mathrm{F}\Phi + \mathrm{R}T \ln c_k + \mathrm{R}T \left(\ln f_k - z_k z_n^{-1} \ln f_n\right) + \mathrm{R}T(\ln a_k^{\ominus} - z_k z_n^{-1} \ln a_n^{\ominus}), \quad [8]$$

where the electrostatic potential Φ in the electrolyte solution is defined with respect to an arbitrary negative ionic species n present in the electrolyte solution.[1] The anion of the supporting electrolyte is chosen as the reference species n, since it does not take part in any faradaic reaction at the electrodes in lithium ion batteries. Furthermore, the charge number of the ionic species k is denoted by z_k, the activity coefficient of the ionic species k by f_k, the Faraday constant by F, the gas constant by R, the temperature by T, and the proportionality constant for the secondary reference state of the ionic species k by $a_k^{\ominus}$. In addition, the following definition for the electrochemical potential of the reference species n is used according to Newman and Thomas-Aleya[1]

$$\tilde{\mu}_n = z_n \mathrm{F}\Phi + \mathrm{R}T \ln c_n. \quad [9]$$

In this framework, the activity coefficient and the proportionality constant of the reference species is included in the electrochemical potential of the ionic species k, as can be seen in Eq. 8, and thus does not occur in Eq. 9. In the following, the perchlorate ion ClO_4^- is chosen as reference species n. As a result, combining Eq. 1 and 8, the electrochemical potentials of lithium and ferrocenium ions can be written as

$$\tilde{\mu}_{Li^+} = z_{Li^+}\mathrm{F}\Phi + \mathrm{R}T \ln c_{Li^+} + \mathrm{R}T \ln f_{LiClO_4}^2 + \mu_{LiClO_4}^{\ominus}, \quad [10]$$

$$\tilde{\mu}_{Fc^+} = z_{Fc^+}\mathrm{F}\Phi + \mathrm{R}T \ln c_{Fc^+} + \mathrm{R}T \ln f_{FcClO_4}^2 + \mu_{FcClO_4}^{\ominus}. \quad [11]$$

The standard chemical potentials of lithium perchlorate

$$\mu_{LiClO_4}^{\ominus} = \mathrm{R}T \ln \left(a_{Li^+} a_{ClO_4^-}\right) \quad [12]$$

and ferrocene perchlorate $\mu_{FcClO_4}^{\ominus}$

$$\mu_{FcClO_4}^{\ominus} = \mathrm{R}T \ln \left(a_{Fc^+} a_{ClO_4^-}\right) \quad [13]$$

defined according to Newman and Thomas-Alyea, are independent of the electrolyte composition but are a function of additional state variables such as temperature and pressure. The mean binary activity coefficients of lithium perchlorate and ferrocene perchlorate are given by $f_{LiClO_4}^2$ and $f_{FcClO_4}^2$ as defined in Eq. 1. Therefore, using Eq. 10 and 11, Eq. 7 can be expressed as,

$$\mathrm{F}U = \mathrm{R}T \ln \left(c_{Fc^+} f_{FcClO_4}^2\right)|_{WE} + \Delta_R G|_{WE} - \mu_{Fc}|_{WE} - \mathrm{R}T \ln \left(c_{Li^+} f_{LiClO_4}^2\right)|_{RE} + \mathrm{F}(\Phi|_{WE} - \Phi|_{RE}) + \mu_{Cell}. \quad [14]$$

Here, the standard chemical cell potential μ_{Cell} includes the chemical potential of lithium μ_{Li} as well as the standard chemical potentials of lithium perchlorate $\mu_{LiClO_4}^{\ominus}$ and ferrocenium perchlorate $\mu_{FcClO_4}^{\ominus}$

$$\mu_{Cell} = (\mu_{Li}|_{RE} - \mu_{LiClO_4}^{\ominus}|_{RE} + \mu_{FcClO_4}^{\ominus}|_{WE}). \quad [15]$$

The potential drop in the electrolyte is described by the term $\Phi|_{WE} - \Phi|_{RE}$. From Eq. 14, the cell potential U can also be written as

$$U = U_{Ref} - \mathrm{R}T/\mathrm{F} \ln(c_{Li^+} f_{LiClO_4}^2), \quad [16]$$

where the reference potential U_{Ref} includes all remaining terms which are independent of the $LiClO_4$ concentration.

$$U_{Ref} = [\mathrm{R}T/\mathrm{F} \ln(c_{Fc^+}/c_{Fc}) + \Delta_R G + \mathrm{R}T/\mathrm{F} \ln(f_{FcClO_4}^2) - \mathrm{R}T/\mathrm{F} \ln(f_{Fc})]|_{WE} + \mu_{Cell} + \Delta\Phi. \quad [17]$$

If the ferrocene concentration is kept constant for different $LiClO_4$ concentrations, U_{Ref} can be shown to be constant as will be discussed in detail in section Reference potential.

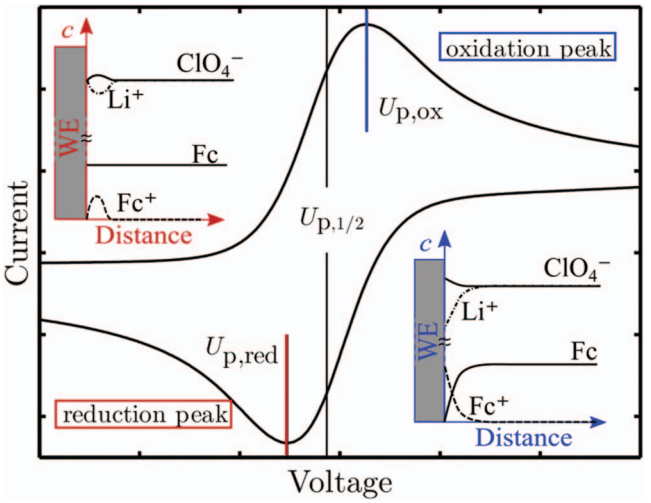

Figure 2. Concentration profiles in the vicinity of the Working Electrode (WE) for the components dissolved in the electrolyte solution at the oxidation peak (blue) and the reduction peak (red) of a cyclic voltammogram.

In summary, the relation given in Eq. 16 is the basis for the determination of the mean molar activity coefficient by cyclic voltammetry experiments which requires a constant ferrocene concentration throughout a measurement series while the $LiClO_4$ concentration is varied. As the obtained cell potential U is given by a constant U_{Ref} and an expression containing the activity coefficient of $LiClO_4$, the latter quantity can be determined mathematically.

Potential of oxidation and reduction peaks.—In the following, possible influences on the peak positions of a cyclic voltammogram are analyzed. While in the *Results and Discussion* part half wave potential $U_{p,1/2}$ versus the lithium reference electrode are used as reference point (U in Eq. 16), in this section we evaluate to which extent oxidation and reduction peak potentials may be affected by, e.g., the scan range. In general, the positions of oxidation and reduction peaks are defined by the ratio of ferrocenium to ferrocene at the WE. Idealized concentration profiles at both peaks are shown in Figure 2. At the oxidation peak, ferrocene is depleted at the WE while at the reduction peak the ferrocenium ion concentration approaches zero at the WE. In addition, this ratio is also the basic boundary condition for the boundary value problem as described, e.g., in Bard and Faulkner.[14] This becomes clearer, if Eq. 16 and Eq. 17 are reformulated to

$$c_{Fc^+}/c_{Fc} = \exp\left\{\mathrm{F}/\mathrm{R}T \left[(U - \Delta\Phi) - U_0'\right]\right\}. \quad [18]$$

with the formal potential U_0' of the WE with respect to the RE

$$U_0' \equiv \mu_{Cell} - \mathrm{R}T/\mathrm{F} \ln \left(f_{FcClO_4}^2/f_{Fc}\right) - \mathrm{R}T/\mathrm{F} \ln \left(c_{Li^+} f_{LiClO_4}^2\right). \quad [19]$$

Here, in a first approximation, it is assumed that the electrochemical reaction at the WE is always in an equilibrium state (i.e., following Nernstian behavior). In a cyclic voltammetry experiment with a RE, the potential between WE and RE is reduced by the potential drop $\Delta\Phi$ within the electrolyte solution. The cell potential U is time dependent and can be expressed as $U = U_{init} - st$, where s denotes the constant scan rate, U_{init} the initial cell potential and t the time. Based on this boundary condition, the following theoretical relations can be derived for the oxidation peak only in the first cycle.[14] The theoretical peak position $U_{p,ox}$ for the first cycle is given by

$$U_p = U_0' + \mathrm{R}T/\mathrm{F} \ln (D_{Fc}/D_{Fc^+})^{1/2} - 1.109\mathrm{R}T/\mathrm{F} \quad [20]$$

and the peak current by

$$I_{p,ox} = 2.69 \cdot 10^5 \mathrm{A}(D_{Fc})^{1/2} c_{Fc}^0 s^{1/2}. \quad [21]$$

for a perfectly reversible Nernstian couple. The diffusion coefficient of ferrocene is denoted by D_{Fc} and the diffusion coefficient of the

Table I. Peak separation for Nernstian system with variable positive vertex potentials $U_{reverse}$.

$\lvert U_{p,ox} - U_{reverse}\rvert$ [mV]	171,5	271,5	∞
$U_{p,ox} - U_{p,red}$ [mV]	58,3	57,8	57,0

ferrocenium ion by D_{Fc^+}. The ferrocene concentration in the bulk of the electrolyte solution is indicated by c^0_{Fc}. Since ferrocenium ions are the minor species in the supporting electrolyte solution, they can be approximated by the pure diffusion problem with the ionic diffusion coefficient D_{Fc^+}.[1] The connection of the mean molar activity coefficient with the oxidation peak position for a single forward scan becomes clear in Eq. 16. If the measured potential U in Eq. 16 is only a function of the term $\ln(c_{Li^+} f^2_{LiClO_4})$ and if all other terms are constant, it is possible to determine the mean activity coefficient from the peak potential.

For a cyclic voltammogram of a reversible (i.e., Nernstian) redox couple, it is possible to derive a theoretical value for the peak separation defined by the potential difference between the peak potentials for oxidation $U_{p,ox}$ and reduction $U_{p,red}$. In general, the theoretical peak separation depends on the potential difference between the peak potentials $U_{p,i}$ and the vertex potentials at which the scan rate is reversed $U_{reverse,i}$. The theoretical values for a reversible Nernstian couple are shown in Table I.[14]

Concluding from Table I, a peak separation of 57 mV within 1 mV would be expected for reversible Nernstian couples if the difference between vertex and the peak potential is >300 mV. This theoretical value for the peak separation can be used to evaluate the quality of experimental data.

Reference potential.—To be able to use cyclic voltammetry in combination with the shown experimental setup for the determination of mean molar activity coefficients $f_{LiClO_4}(c)$, it is necessary that the reference potential U_{Ref} is independent of the supporting electrolyte salt concentration c. Therefore, it is important to get a detailed understanding of the characteristics of individual terms contributing to the reference potential U_{Ref} in Eq. 17. As discussed before, the logarithmic ratio of ferrrocenium to ferrocene at the WE, the first of the terms in Eq. 17, defines the theoretical positions of oxidation and reduction peaks and they are independent of the supporting electrolyte concentration.

Next, the $\Delta_R G$ term will be examined. For the derivation of the theoretical peak positions and the peak separation, it is assumed that the system is only limited by mass transport, i.e., infinitively fast kinetics are assumed. However, in reality, kinetic effects have to be considered, as they also influence the peak separation and, therefore, the peak positions. If the reaction Gibbs energy $\Delta_R G$ is not negligibly small, it can be approximated by the kinetic overpotential η, which describes the deviation from the equilibrium potential at the specific condition.[1] In this case, the peak separation is linked to the parameter Ψ defined and tabulated in Bard and Faulkner:[14]

$$\Psi = \frac{(D_{Fc^+}/D_{Fc})^{\alpha/2} k_0}{(\pi D_{Fc^+} \mathrm{F}/\mathrm{R}T\, s)^{1/2}}. \qquad [22]$$

Here, α denotes the transfer coefficient in the Butler-Volmer equation and k_0 the standard rate constant of the electrochemical reaction. According to Eq. 22, the peak separation depends on the diffusion coefficient ratio and the standard rate constant, whereby both quantities may be a function of the supporting electrolyte concentration. A decrease of the value of the parameter Ψ due to slow kinetics, results in an increase in the peak separation, which is distributed symmetrically between oxidation and reduction peaks as shown, e.g., by Table 6.5.2 in Bard and Faulkner.[14] To decrease the influence of the non-Nernstian redox couple response (i.e., of finite kinetics), the half-wave potential $U_{p,1/2} = 1/2(U_{p,ox} + U_{p,red})$ can be used as a reference point instead of the oxidation or reduction peak positions (see Figure 2). For the half-wave potential, the symmetric potential shifts of oxidation and reduction peaks cancel out.

The next term in Eq. 17 is the mean molar activity coefficient of ferrocenium perchlorate $\ln(f_{FcClO_4})|_{WE}$, which is assumed to be constant in this work. This assumption is based on the original publication by Gritzner and Kuta.[15] In their publication, the authors argue that the activity of the ferrocene – ferrocenium species is independent of the surrounding solution. An even stronger argument for the constancy of the term $\ln(f_{FcClO_4})|_{WE}$ is its influence on oxidation and reduction peak positions. As ferrocenium ions only exist at the oxidation peak a possible contribution by the $\ln(f_{FcClO_4})|_{WE}$ term can only occur for this peak. Thus, when the $LiClO_4$ concentration is varied between experiments, a varying contribution to the oxidation peaks should be observable compared to the reduction peak. Experimental results shown later will prove that oxidation and reduction peaks behave in a completely identical manner. As the activity coefficient of the uncharged ferrocene is one, the fourth term in Eq. 17 can be assumed constant as well. The fifth term on the right-hand-side of Eq. 17, the chemical potential of the cell, μ_{Cell}, as defined in Eq. 15, depends on the used electrode materials and the electrolyte solution, which is generally constant for isothermal and isobaric conditions.

So far, all discussed terms deal with the electrolyte composition in the vicinity of the electrodes. In contrast to those, the last term in Eq. 17, the potential drop $\Delta\Phi$ describes the potential difference in the electrolyte between working and reference electrode. The potential field in such an electrolyte solution is described by

$$\nabla\Phi = \mathrm{R}T/\mathrm{F}\nabla \ln c_{ClO_4^-} - \boldsymbol{i}/\kappa - \mathrm{R}T/\mathrm{F}\xi, \qquad [23]$$

with

$$\xi = t_{Li^+}\nabla \ln\left(c_{Li^+} c_{ClO_4^-} f^2_{LiClO_4}\right) + t_{Fc^+}\nabla \ln\left(c_{Fc^+} c_{ClO_4^-} f^2_{FcClO_4}\right), \qquad [24]$$

which describes the current transport in concentrated electrolyte solutions derived from the Stefan-Maxwell approach

$$\mathrm{F}\boldsymbol{i}/\kappa = -\left(\sum_{k=1}^{n} t_k/z_k \nabla\tilde{\mu}_k\right) \qquad [25]$$

using Eqs. 9–11.[1] Here, the current density is denoted by $\boldsymbol{i}$, the conductivity of the electrolyte solution by κ, and the transference numbers of lithium and ferrocenium ions by t_{Li^+} and t_{Fc^+}, respectively. A similar system is also discussed for example in Newman and Thomas-Alyea.[1] Using a one-dimensional approximation of the given setup and performing an integration along a path between RE and WE, it is possible to get an approximation for the potential drop between RE and WE

$$\Delta\Phi = \mathrm{R}T/\mathrm{F}\ln\left(c_{ClO_4^-}|_{WE}/c_{ClO_4^-}|_{RE}\right) - R_\Omega \boldsymbol{i} A - \mathrm{R}T/\mathrm{F}\int_{RE}^{WE}\xi \mathrm{d}x. \qquad [26]$$

The ohmic resistance of the electrolyte solution is denoted by R_Ω and the current by $\boldsymbol{i}A$. In this formulation, the third term on the right-hand-side of Eq. 26 is not integrated, yet. The first term on the right hand side is zero since the perchlorate ion concentration is approximately constant in the entire electrolyte solution for oxidation as well as reduction peaks as indicated in Figure 2. The second term $R_\Omega \boldsymbol{i} A$ describes the potential drop within the electrolyte solution as a result of the current. Although the current between WE and RE is negligibly small, an ohmic potential is included in the cell potential U as a result of the current flowing between WE and CE. The so-called effect of uncompensated resistance between RE and WE thus also leads to an increased peak separation.[14] This effect is particularly pronounced for small supporting electrolyte concentrations since the resistance of the electrolyte solution is very large in this case. The increase in peak separation is not completely symmetric, since the peak currents at oxidation and reduction peak are usually not equal in a cyclic voltammogram. In order to reduce the effect of uncompensated resistance, the current between WE and CE electrode has to be minimized. Experimental parameters influencing the current are the scan rate and

the ferrocene concentration, as indicated in Eq. 21, so that low scan rates and/or ferrocene concentrations are desired. Furthermore, the potential drop $\Delta\Phi$ in the electrolyte is also influenced by the third term in Eq. 26, which describes the concentration overpotential resulting from concentration gradients within the electrolyte. In general, concentration gradients have to be considered only in the vicinity of the WE. The RE compartment is separated from the WE, thereby guaranteeing uniform lithium and perchlorate ion concentration profiles. Additionally, the polarization times are short enough (on the order of 10^2 s for the scan rates and potential windows used in our study), so that concentration gradients developing at the WE do not penetrate far into the bulk region of the electrolyte solution. As a result of small concentration variations within the electrolyte, it is valid to assume constant transference numbers for the integration of ξ in Eq. 26

$$R\mathit{T}/F\int_{RE}^{WE}\xi dx = R\mathit{T}/F\Big[t_{Li^+}\ln\left\{\left(c_{Li^+}f_{LiClO_4}^2\right)_{WE}\left(c_{Li^+}f_{LiClO_4}^2\right)_{RE}^{-1}\right\} + t_{Fc^+}\ln\left\{\left(c_{Fc^+}f_{FcClO_4}^2\right)_{WE}\left(c_{Fc^+}f_{LiClO_4}^2\right)_{RE}^{-1}\right\}\Big] \quad [27]$$

whereby contributions of the perchlorate ions in the integral cancel out due to its uniform concentration profile (i.e., small changes in concentration compared to its overall concentration). The last term depending on the transference number of the ferrocenium ion in Eq. 27 can also be neglected, since the transference number of the minor species in a supporting electrolyte solution is approximately zero for a high ratio of supporting electrolyte to minor component. Such a high ratio also has a positive effect on the first term of the Eq. 27 since the concentration difference of lithium ions between WE and RE is also minimized. Concluding, a minimal ratio of ferrocenium ions, respective ferrocene, to supporting electrolyte is also advantageous to avoid concentration overpotentials. This is of course most critical for small concentrations of supporting electrolyte. It is emphasized that the concentration overpotential does not influence both peaks symmetrically. At the oxidation peak, the concentration difference for lithium as well as ferrocenium ions are the highest, resulting in a maximum concentration overpotential. On the contrary, the concentration differences of supporting electrolyte ions between RE and WE are negligibly small at the reduction peak. As a result, concentration overpotentials influence oxidation but not reduction peaks. As for all non-symmetric terms, this has to be considered if the half-wave potential is used for the determination of the mean activity coefficient, particularly for small supporting electrolyte concentrations.

Theoretical behavior of the mean molar activity coefficient of binary salts.—If all above mentioned theoretical assumptions are valid and if the experimental conditions are such that all of the above approximations are met, the reference potential U_{Ref} in Eq. 16 can be considered sufficiently independent of the lithium salt concentration, so that the logarithmic activity coefficient can be obtained from the variation of the cell potential U vs. the lithium salt concentration by means of Eq. 16. A well-known theoretical derivation for the logarithmic activity coefficient f_{LiClO_4} is the so-called Debye-Hückel law.[14,16] Thus, in the following paragraphs, different formulations as well as extensions of the Debye-Hückel law are compared. The listed approximations for the respective concentration regions provide a theoretical framework for a comparison with the measurements and thereby offers a means to validate the experimental results. According to the Debye-Hückel law, the theoretical behavior of the mean molar activity coefficient f_{LiClO_4} can be described by

$$\ln f_{LiClO_4} = -\left|z_{Li^+}z_{ClO_4^-}\right| A\sqrt{I}\left(1+B\dot{a}\sqrt{I}\right)^{-1}, \quad [28]$$

where A, B, and $\dot{a}$ are defined below, and where I is the ionic strength of the electrolyte defined as

$$I = \frac{1}{2}\sum_{k=1}^{m} z_k^2 c_k \quad [29]$$

with $m = 3$ dissolved ionic species in our case (Li^+, ClO_4^-, and Fc^+). The parameters A and B are defined as

$$B = \left(2e^2N_A\right)^{1/2}(\varepsilon_0\varepsilon_R kT)^{-1/2} = \varepsilon_R^{-1/2}\cdot 2.914\cdot 10^9 dm^{\frac{1}{2}}mol^{-\frac{1}{2}}, \quad [30]$$

$$A = e^2(8\pi\varepsilon_0\varepsilon_R kT)^{-1}B = \varepsilon_R^{-3/2}\cdot 817.1L^{\frac{1}{2}}mol^{-\frac{1}{2}}. \quad [31]$$

In Eqs. 28–31, the minimal distance between two ionic species is denoted by $\dot{a}$, the relative permittivity by ε_R, the permittivity of vacuum by $\varepsilon_0 = 8.854\cdot 10^{-12}$ F, m^{-1}, the electronic charge by $e = 1.602\cdot 10^{-19}$ C, the Avogadro constant by $N_A = 6.022\cdot 10^{23}\,mol^{-1}$, and the gas constant by $R = 8.314\,J\,mol^{-1}K^{-1}$. Eq. 28 can also be approximated by the Debye-Hückel limiting law[17]

$$\ln f_{LiClO_4} = -\left|z_{Li^+}z_{ClO_4^-}\right| A\sqrt{I} \quad [32]$$

applicable for low ionic strengths which will be discussed in detail in the Results and discussion section. For electrolyte solutions with higher ionic strengths, the Debye-Hückel law (Eq. 28) is often extended by a linear term[17]

$$\ln f_{LiClO_4} = -\left|z_{Li^+}z_{ClO_4^-}\right| A\sqrt{I}\left(1+B\dot{a}\sqrt{I}\right)^{-1} + x_1 I. \quad [33]$$

This is an empirical extension accounting for effects like short range interactions between ions and the solvent, dispersion forces between ions, or ion association. A detailed discussion of this topic can be found, e.g., in Wright.[17] An n^{th} -order polynomial with respect to the concentration instead of ionic strength is frequently used by Newman and Thomas-Alyea to account for effects which are not included in the Debye-Hückel theory[1]

$$\ln f_{LiClO_4} = -\left|z_{Li^+}z_{ClO_4^-}\right| A\sqrt{I}\left(1+B\dot{a}\sqrt{I}\right)^{-1} + y_1 c + y_2 c^{3/2} + y_3 c^2 + \ldots. \quad [34]$$

In this work, the extended form of the Debye-Hückel law given by Eq. 33 is used. Fits with higher order terms according to Eq. 34 were found to over-interpret experimental results.

Results and Discussion

Selection of experimental procedure.—As the parameters of the CV measurements influence the validity of theoretical assumptions and simplifications, it is necessary to identify a proper set of measurement conditions to fulfil the requirements described in the theoretical part of this work, mostly the small ferrocene concentration in comparison with the $LiClO_4$ salt. Figure 3 shows the steady-state CVs ($\geq 2^{nd}$ scan) with 0.05 and 0.10 mM concentrations of ferrocene in 2 mM $LiClO_4$ at scan rates of 10 and 20 mV/s. All curves show reversible oxidation and reductions peaks of the ferrocene/ferrocenium couple at ~3.51 and ~3.43 V, respectively. Following the arguments in the *Theory* section, the smaller ferrocene concentration of 0.05 mM was used for the following experiments in order to satisfy the requirement of a small c_{Fc} to c_{LiClO_4} ratio, thereby avoiding parasitic effects such as diffusion overpotentials. Additionally, small ferrocene concentrations result in small currents and thus small ohmic drops in the electrolyte phase; they also allow that the ionic strength can be described sufficiently accurately by the concentration of the lithium salt only. Extraction of oxidation and reduction peak potentials was done by calculation of maxima and minima of fifth order polynomials which were fitted through data points in a range of ± 50 mV around the peaks. Due to the sensitivity of this procedure on the peak sharpness, the larger scan rates of 20 mV/s, showing higher oxidation and reduction currents, are used subsequently. For the same reason, the ferrocene concentration is not reduced below 0.05 mM. All following experiments have been conducted using the just determined set of measurement conditions, viz., a scan rate of 20 mV/s and a ferrocene concentration of 0.05 mM.

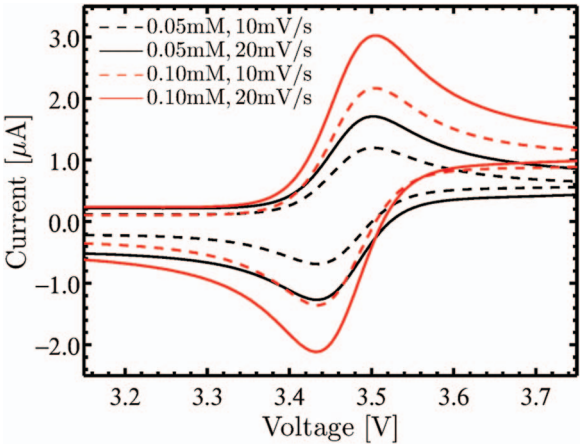

Figure 3. Steady-state CVs at two different scan rates (10 mV/s, dashed line and 20 mV/s, solid line) for two different ferrocene concentrations ($c_{Fc} = 0.05$ mM, black and $c_{FC} = 0.10$ mM, red) in 2 mM $LiClO_4$ in EC:DEC (1:1, w:w) with positive and negative potential limits of 2.5 and 4 V (85% online IR correction were used).

Ohmic drop compensation and correction.—In this Section, the goal is to find a method to best correct the CVs for IR losses, which is required for the later detailed analysis. Figure 4 shows an example for the influence of different types of IR correction on the peak positions. Without IR correction, oxidation and reduction peak potentials in a 1 mM $LiClO_4$ electrolyte with 0.05 mM ferrocene are 3.550 and 3.428 V respectively. Ferrocene oxidation and reduction peak potentials of 3.531 V and 3.443 V are obtained if the raw data are IR corrected after the measurement according to

$$U_{i,\text{corr}} = U_{i,\text{meas}} - I_{i,\text{meas}} \cdot R_{\text{RE-WE}}. \quad [35]$$

whereby $R_{\text{RE-WE}}$ was obtained by impedance measurements prior to the CV scans. In the following, this method is called *post IR correction*, according to its execution after the measurement. As oxidation and reduction currents are different (2.8 μA and 2.3 μA respectively), the post IR correction has different impacts on oxidation and reduction peak potentials, resulting in a non-symmetric behavior which can be observed in Figure 4.

For electrolyte solutions with RE-WE resistances in the kΩ range, the effective potential in the cyclic voltammogram is not truly linear with time anymore. This behavior can be circumvented by online IR correction, i.e., during the CV scans, using a certain percentage of the uncompensated resistance as explained by Bard and Faulkner.[14] Essentially, the scan rate is adjusted continuously during the scan, resulting in a linear effective potential vs. time behavior, although the applied potential is non-linear.[18] As oscillations occur for online IR corrections close to 100% of the total uncompensated resistance, $R_{\text{RE-WE}}$, caused by the measurement hardware, it was only possible to correct for 85% of the ohmic drop. As a result, a combined IR correction, consisting of an online IR correction and a subsequent post IR correction is introduced in the following and will be referred to as *85/15 combined IR correction*, where 85 denotes the percentage of online IR corrected resistance and 15 the percentage of post IR corrected resistance. Figure 4 shows the effect exemplarily for a 75/25 combined IR correction, giving a peak potential of 3.526 V for oxidation and 3.447 V for reduction peak potentials, respectively. Although both cases, 100% post IR correction and a 75/25 combined IR correction, theoretically account for the same total ohmic drop, a difference in peak positions of ∼5 mV is observed between both methods. This shows the importance of online over post IR correction and raises the question of remaining uncertainties for the combined IR correction.

As a full online IR correction, i.e., 100/0 combined IR correction, cannot be realized, CVs with four different percentages of online IR correction were measured in a 0.1 mM $LiPF_6$ electrolyte (Figure 5)

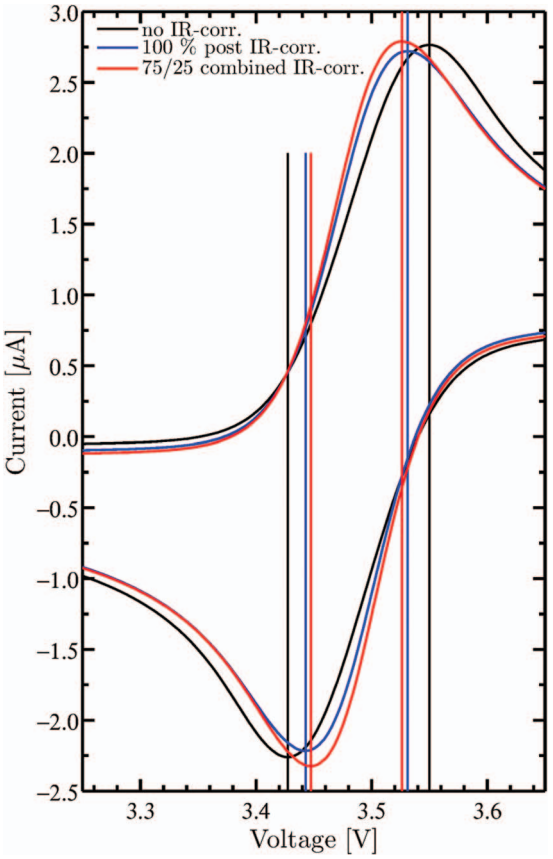

Figure 4. CVs showing the influence of IR correction on oxidation and reduction peak positions with 0.1 mM ferrocene at 20 mV/s in 1 mM $LiClO_4$ in EC:DEC (1:1, w:w) with positive and negative potential limits of 2.5 and 4 V: no IR correction (black), 100% post IR correction (blue), and 75/25 combined online/post IR correction (red). The value of $R_{\text{RE-WE}}$ determined by AC impedance was 6.9 kΩ.

to validate the following analysis procedure. This small concentration with the highest solution resistance is chosen to best illustrate the effect. Cross and plus symbols in Figure 5 correspond to oxidation and reduction peak potentials which are only online IR corrected. Subsequent post IR correction of these potentials by the remaining resistance, referred to as combined IR correction, results in oxidation and reduction potentials indicated by circles and triangles, respectively. The peak potentials resulting from a pure online IR correction and the combined IR corrections are extrapolated in Figure 5 to the theoretical 100% online IR correction based on the peak potential values for 25%, 45%, 65% and 85% online correction. The data are well represented by linear extrapolation lines as shown in Figure 5, with an interception point close to 100% online IR correction. For the extreme example shown in Figure 5, the peak potentials obtained from a 85/15 combined IR correction still show a small deviation of ∼3.5 mV from the extrapolated 100% online IR corrected value. Therefore, for all the following measurements, at least two different ratios of combined IR correction were used to determine peak potentials by extrapolating to 100% online IR correction; this methodology will be referred to as *100% extrapolated IR correction*. It should be noted, however, that for concentrations above 5 mM, the latter correction leads to negligibly small differences compared the value obtained from a 85/15 combined IR correction (<1 mV).

Data selection.—A quality measure for the obtained oxidation and reduction potentials is the peak separation. For reversible processes with fast electrode kinetics (Nernstian behavior), the theoretical peak

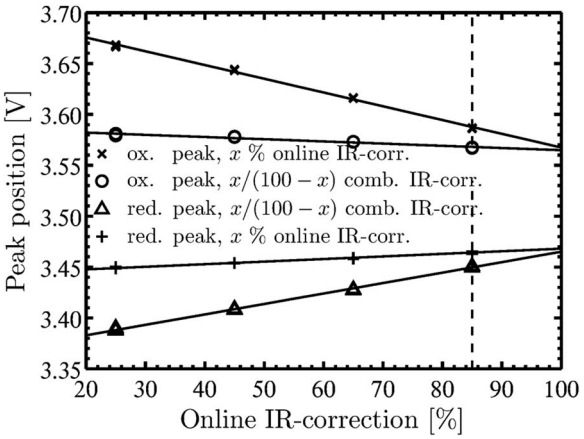

Figure 5. Oxidation/reduction peak potentials versus different applied percentages of online IR corrections without remaining post IR correction (cross/plus symbols) and with additional post IR correction (circle/triangle symbols) corresponding to the combined IR correction method. Conditions: 0.1 mM $LiPF_6$ in EC:DMC (1:1, w:w) with 0.05 mM ferrocene at 20 mV/s with positive and negative potential limits of 2.5 and 4 V ($R_{RE\text{-}WE} = 72$ kΩ).

separation as given by Table I should be 57–58 mV, as the difference between peak and the vertex potentials are larger than 300 mV.

For all measured $LiClO_4$ concentrations, the potential differences between oxidation and reduction peaks are plotted in Figure 6. To show reproducibility, the peak separation data are shown for three independent measurement series. In the measurement series three (red symbols), extrapolated values exist only for concentrations between 0.5 and 20 mM and above 20 mM only combined IR corrections are shown. Figure 6 depicts constant and identical peak separations for each series at concentrations above 5 mM, independent of the IR compensation method. For concentrations below 5 mM $LiClO_4$, the peak potential increases to 90–100 mV for the extrapolated IR correction values at the lowest concentration of 0.1 mM $LiClO_4$. From the constant peak separation of all measurement series for concentrations above 5 mM it is concluded, that all non-ideal effects discussed in the Theory section which influence the peak potentials are negligible. The first measurement series (green symbols) shows a shift of all measured peak separations by ∼5 mV compared to measurement two and three. This was identified as an experimental artefact caused by not flame annealing of the Au working electrode, thereby not removing thin oxide layers on the working electrode. The latter reduces the rate constant k_0 of the outer electron transfer[19] of the ferrocene/ferrocenium couple, which depends on the electron tunneling length, i.e., the thickness of

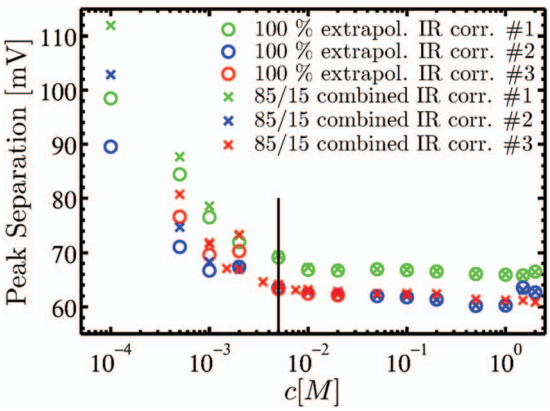

Figure 6. Peak separation of three measurement series with extrapolated values of series two and three, according to method depicted in Figure 5. The solid line indicates a concentration of 5 mM. Conditions: $LiClO_4$ of specified concentration in EC:DEC (1:1, w:w) with 0.05 mM ferrocene at 20 mV/s with positive and negative potential limits of 2.5 and 4 V.

the oxide layer on the gold surface. A smaller rate constant k_0 results in an increased peak separation according to Eq. 22. Nevertheless, even for the experiments conducted with properly annealed Au working electrodes (red and blue symbols in Figure 5), a deviation of ∼5 mV from the expected peak separation (57–58 mV according to Table I) remains even at $LiClO_4$ concentrations of ≥5 mM, which we believe is due to a limited rate constant k_0, leading to a deviation from the ideal Nernstian behavior. For example, according to Bard and Faulkner,[14] the here observed peak separation of ∼63 mV would be expected for $\Psi = 7$ (see Eq. 22). Based on the measurements by Scholl and Sochaj on the ferrocene/ferrocenium couple on a gold electrode in acetonitrile ($D_R = 2.43 \cdot 10^{-5}$ cm²/s, $D_O = 2.31 \cdot 10^{-5}$ cm²/s, $k_0 = 0.088$ cm/s), Eq. 22 would yield a value of $\Psi = 11.6$, which indeed is reasonably consistent with the peak separation of ∼63 mV at ≥5 mM $LiClO_4$ shown in Figure 5.[20]

For $LiClO_4$ concentrations below 5 mM (at a ferrocene concentration of 0.05 mM), the observed increase in peak separation may be due to several effects and is currently not understood. The kinetic rate constant k_0 and the ratio of diffusion coefficients of ferrocene and ferrocenium depend on the concentration of $LiClO_4$ as explained in the theoretical part of this work. Thus, the ratio between ferrocenium and ferrocene diffusion coefficients which affects the peak separation (see Eq. 22), was shown to depend on the supporting electrolyte concentration by Wang et al.[21] and Ruff et al.[22] However, a quantitative estimation is not possible, as no literature values exist for our electrolyte. Similarly, the dependence of the reaction rate constant k_0 was shown to depend on the concentration of the supporting electrolyte by Peter et al. for the ferro/ferri-cyanide couple.[23] In the same publication, the effect of ion pairing is also mentioned as an explanation for the non-ideal behavior of a cyclic voltammogram. A similar concept is discussed in Redepenning et al.[24]

In addition, the ratio of ferrocene to supporting electrolyte may introduce a diffusion overpotential, which would affect oxidation and reduction peak potentials asymmetrically (compare Eq. 27). The concentration overpotential estimated by Eq. 27, however, only partly explains the increase in peak separation. For example, a decrease in peak separation of ∼2 mV is expected for a 1 mM $LiClO_4$ concentration, if the concentration overpotential is subtracted from the oxidation peak potential. This low value is a result of the chosen experimental setup with a minimal ferrocene to $LiClO_4$ concentration ratio (1/20 at 1 mM $LiClO_4$). An obvious trend is only visible for the smallest $LiClO_4$ concentration of 0.1 mM $LiClO_4$, where the half peak potential is clearly shifted towards the oxidation peak as a result of the non-symmetric behavior of the concentration overpotential as explained in the Theory section.

We believe that the most likely explanation for the increase in peak separation is a supporting electrolyte concentration dependence of the rate constant k_0. Nonetheless, for concentrations below 5 mM, a combination of all of the described effects may be the case. As a consequence of this uncertainty, we will only consider concentrations above 5 mM $LiClO_4$ for the below described evaluation of the thermodynamic factor from our data, even though data derived from smaller concentrations are still plotted for comparison.

Parameter extraction.—In Figure 7, the negative values of the measured oxidation peak, reduction peak, and half-wave potentials, U, recorded at a series of $LiClO_4$ concentrations are subtracted by $RT/F \ln(c_{Li^+})$ and are plotted versus the square root of the $LiClO_4$ concentration. Based on Eq. 16, the thus defined y-axis would correspond to:

$$y_{Axis} \equiv -U - RT/F \ln(c_{Li^+}) = -U_{Ref} + 2\,RT/F \ln\left(f_{LiClO_4}\right) \quad [36]$$

In Figure 7, the previously mentioned constant peak separation as well as its increase for concentrations below 5 mM $LiClO_4$ can be observed, i.e., the difference between oxidation peak potentials (red symbols) and reduction peak potentials (blue symbols) remains constant at ≥5 mM $LiClO_4$ and increases at <5 mM $LiClO_4$. Therefore, for $LiCLO_4$ concentrations of ≥5 mM, the data in Figure 7 can be fitted using Eq. 36 together with Eq. 34 which describes $\ln(f_{LiClO_4})$ versus

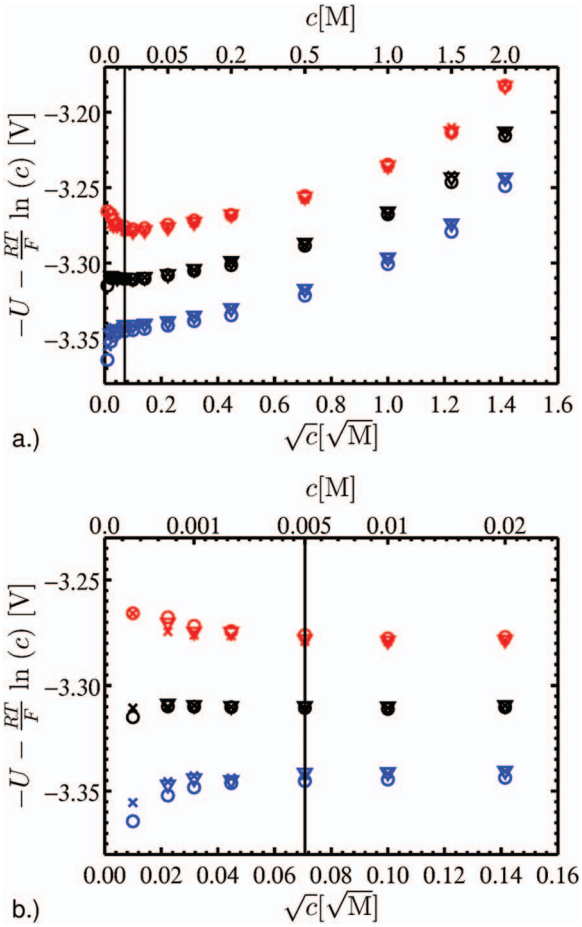

Figure 7. a. Potentials, extrapolated to 100% online IR correction, of reduction peaks (red), half wave positions (black) and oxidation peaks (blue) for three repeat measurement series (circles, crosses, and triangles) versus $LiClO_4$ concentration; b. zoom into the small concentration region; the vertical line marks the concentration of 5 mM $LiClO_4$. Conditions: $LiClO_4$ of specified concentration in EC:DEC (1:1, w:w) with 0.05 mM ferrocene at 20 mV/s with positive and negative potential limits of 2.5 and 4 V.

the $LiClO_4$ concentration, whereby either the oxidation peak, half-wave or reduction peak potentials can be used (each one would result in a different but constant reference potential, U_{Ref}).

For very low concentrations, Eq. 33 simplifies to the Debye-Hückel limiting law given by Eq. 32, which predicts a negative linear slope of the logarithmic mean molar activity coefficient over the square root of concentration. As the concentration is equivalent to the ionic strength as long as the ferrocenium concentration is much smaller than the $LiClO_4$ concentration (note that at 0.001 M $LiClO_4$, the molar ratio of Fc/$LiClO_4$ is 1/20 so that Fc^+/$LiClO_4$ must be <1/20), the slope of the tangent at concentration zero in Figure 7 should be negative and proportional to the Debye Hückel parameter A. Inspecting Figure 7b, it is clear that this expected behavior is only observed for the oxidation peak potentials, but not for the reduction peak potentials or the half-wave potentials, probably caused by the unknown peak separation at ≤5 mM $LiClO_4$ (see Figure 6), which as discussed above does not allow a meaningful analysis of the data at concentrations substantially below 5 mM $LiClO_4$. Nevertheless, this raises the question below which concentration the Debye-Hückel limiting law behavior would be expected to occur in the here used aprotic electrolytes. A way to estimate the concentration range in which the simplified Debye-Hückel behavior is expected is the comparison of the two terms in the denominator of the first term on the right-hand-side of Eq. 33: the Debye-Hückel limiting behavior is expected as long as $B\dot{a}\sqrt{I} \ll 1$. To approximate up to which concentration the limiting law and the Debye-Hückel equation give the same result, we assume a maximum deviation between both descriptions of 5%, which corresponds to $B\dot{a}\sqrt{I} = 0.05$. Parameter $\dot{a}$ in Eq. 33 corresponds to the distance of closest approach[16] and parameter B simply depends on the relative permittivity of the solvent (see Eq. 30). The relative permittivity of the electrolyte ($LiClO_4$ in EC:DEC, 1:1 w:w) was measured in a coaxial cell setup using impedance spectroscopy, yielding a value of $\varepsilon_R \approx 35 \pm 3$, which is consistent with that reported for a similar electrolyte ($LiClO_4$ in PC:DEC, 1:1 w:w) reported by Ding et al.[25] A reasonable estimate for the distance of closest approach in our aprotic solvent is $\dot{a} \sim 1$ nm.[16] It follows, that for $\dot{a} \sim 1$ nm and $\varepsilon_R \approx 35$ the approximate concentration up to which the Debye-Hückel limiting law deviates at most by 5% from the Debye-Hückel equation is ~0.1 mM $LiClO_4$, which is way below the range of our measurements. In comparison, the Debye-Hückel limiting law should be observable up to concentrations of ~2–3 mM for aqueous systems ($\varepsilon_R \approx 80$, $\dot{a} \sim 0.3$ nm).[16]

Table II. Fitting parameters and their standard deviation extracted from the fits of the measured half-wave potentials with Eq. 36 and Eq. 33, as shown in Figure 8, illustrating the influence of the chosen relative permittivities of 35 and 40.

ε_r [−]	U_{Ref} [V]	$\dot{a}$ [nm]	x_1 [−]	R^2 [−]
35	3.3079 ± 0.0042	12.8 ± 23.4	0.907 ± 0.016	0.996
40	3.3077 ± 0.0047	13.7 ± 25.6	0.907 ± 0.016	0.996

In summary, for the investigated non-aqueous aprotic electrolyte and within our experimental constraints ($c_{LiClO_4} \geq 5$ mM), it is not possible to get into the range where the Debye-Hückel limiting behavior is expected to apply. Thus, rather than verifying our experimental approach with the Debye-Hückel limiting law, as originally intended, the data points were fitted with Eq. 36, assuming the logarithmic activity coefficient according to Eq. 33 and using a calculated slope A (Eq. 31) based on the measured relative permittivity of the solvent.

Resulting fits of the reformulated half-wave potentials are depicted in Figure 8 with fixed relative permittivities ε_R of the solvent of 35 or 40. A second relative permittivity is shown to analyze the sensitivity of the fit towards the relative permittivity. Although half-wave potentials are used in all further analysis, essentially identical results can be obtained for a fit utilizing the oxidation or reduction peak potentials, as long as the $LiClO_4$ concentrations are ≥5 mM, which is the range in which the peak separation is constant and closely corresponds to its expected value. The extracted fitting parameters are the distance of closest approach $\dot{a}$, the reference potential U_{Ref}, and the slope x_1 of the linear term of the extended Debye-Hückel equation (Eq. 33), all of which are listed in Table II.

For both relative permittivity values, Table II and Figure 8 show an equally good fit, with R^2 values close to 1. Within reasonable error, the same constant reference potentials U_{Ref}, distances of closest approach $\dot{a}$, and linear slope values x_1 are determined. However, while the standard deviations for U_{Ref} and x_1 are quite small (~1.5%), this is not true for $\dot{a}$, which has standard deviations of nearly 200%, indicating the invariance of the fit with respect to $\dot{a}$. Therefore, under the given experimental constraints that data can only be considered trustworthy at $LiClO_4$ concentrations of ≥5 mM, the value of $\dot{a}$ cannot be determined from the fit of measured half wave potentials in EC:DEC based electrolyte and probably in none of the commonly used organics electrolytes. Interestingly, concentrations below 5 mM, even though they have not been used for the fit, are still reasonably well described by the fit. This implies that oxidation and reduction peak potentials are affected more or less symmetrically by the observed increase in peak separation at low $LiClO_4$ concentrations, as was discussed in detail above. It has to be added that an extension of Eq. 33 to higher orders than its linear correlation does not improve the quality of the fit significantly.

Discussion of results.—The methodology to determine the mean molar activity coefficient $f_\pm$ by fitting measured potentials of a

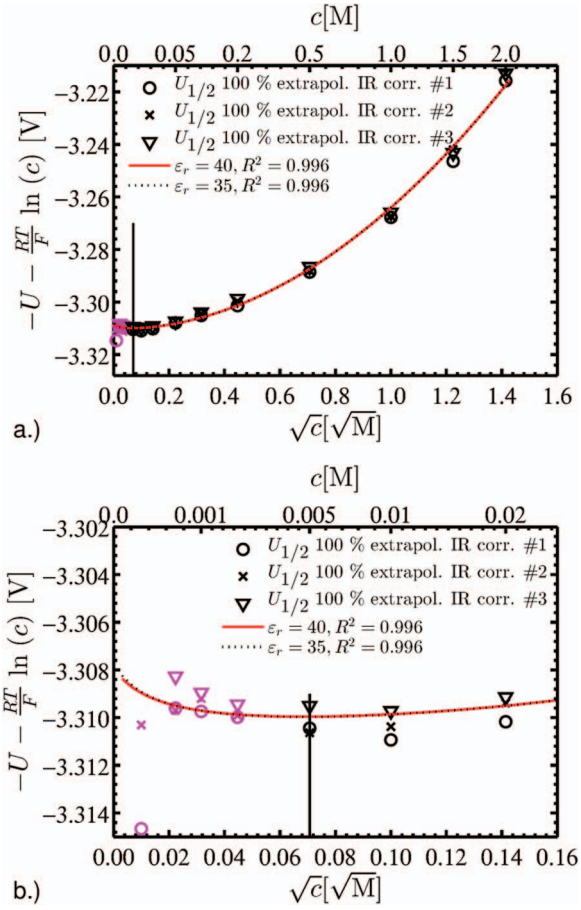

Figure 8. a. Fit of the measured half-wave potentials, U, in the concentration range from 5 mM to 2 M obtained from the 100% extrapol. IR correction (for measurement series three 85/15 combined IR correction values are used above 20 mM 85/15), with Eq. 36 and Eq. 33 to describe the activity coefficient. C; concentrations below 5 mM $LiClO_4$ (magenta symbols) are neglected for the fit. b. Zoom into the low-concentration region. Conditions: $LiClO_4$ of specified concentration in EC:DEC (1:1, w:w) with 0.05 mM ferrocene at 20 mV/s with positive and negative potential limits of 2.5 and 4 V.

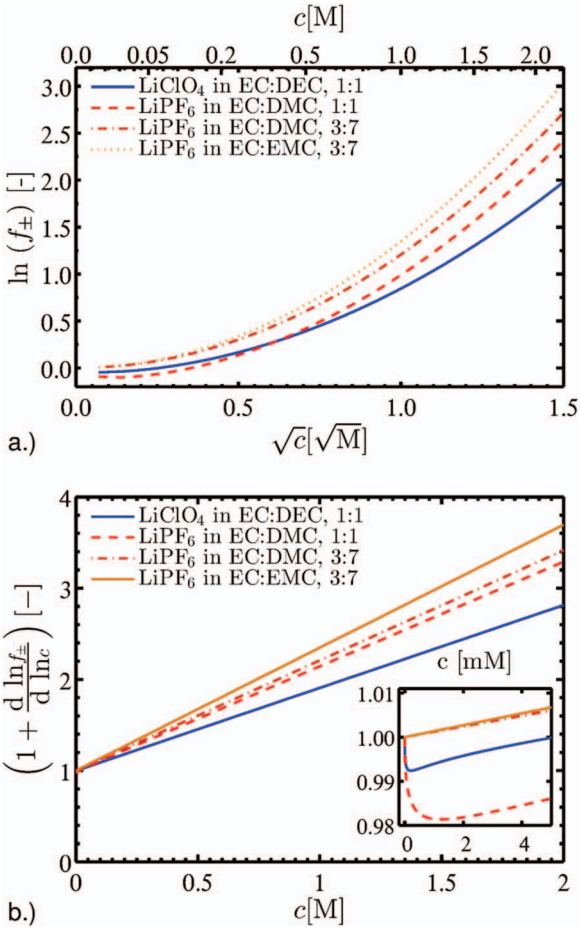

Figure 9. a. Concentration-dependent mean molar activity coefficients of $LiClO_4$ in EC:DEC (1:1, w:w), $LiPF_6$ in EC:DMC (1:1, w:w), $LiPF_6$ in EC:DMC (3:7, w:w), and $LiPF_6$ in EC:EMC (3:7, w:w), obtained from the fitting parameters in Table III for data obtained in a salt concentration range from 5 mM to 2 M, b. Corresponding thermodynamic factors, with a zoom-in view at the low-concentration region.

lithium reference electrode versus half-wave potentials of the ferrocene/ferrocenium redox couple was described in great detail for an exemplary electrolyte with $LiClO_4$ dissolved in a mixture of EC:DEC (1:1, w:w). The same methodology was applied to several more electrolytes in order to generate data which could be compared to the literature: $LiPF_6$ in EC:DMC (1:1, w:w), $LiPF_6$ in EC:DMC (3:7, w:w), and $LiPF_6$ in EC:EMC (3:7, w:w) in a concentration range from 5 mM to 2 M. These electrolytes are representatives of frequently used electrolytes for lithium ion batteries. An overview of measured and fitted parameters of the four electrolytes is given in Table III.

While the fitted parameters U_{Ref} and x_1 yield meaningful values and standard deviations, the fitted $\dot{a}$-values have unreasonably large values and they are plainly nonsensical for $LiPF_6$ in EC:DMC (3:7, w:w) and $LiPF_6$ in EC:EMC (3:7, w:w). This is a result of the insensitivity of the fit to the $\dot{a}$-value, caused by the fact that the lowest considered salt concentration of 5 mM is much too large to observe the Debye-Hückel behavior (see above discussion). Consequently, the natural logarithm of the activity coefficient vs. concentration obtained by inserting the parameters listed in Table III in Eqs. 30, 31, and 33, for the electrolytes with the excessively large and clearly incorrect $\dot{a}$-values depicted in Figure 9a (dotted and dash-dotted red lines), does not go negative at low salt concentrations as would be expected according to the Debye-Hückel limiting law. Owing to the insufficient fitting accuracy of the $\dot{a}$-value, our here presented method does not allow for an accurate description of the value of the activity coefficient, since this would require precise measurements at salt concentrations much less than 5 mM, which experimentally is not possible. This is true not only

Table III. Measured values of ε_r and fitted values for U_{Ref}, $\dot{a}$, and x_1 for four lithium ion battery electrolytes. The salt concentrations ranged from 5 mM to 2 M and the ferrocene concentration was 0.05 mM; CVs were recorded at 20 mV/s between 2.5 and 4 V. Parameters of the LiClO4 containing electrolyte are identical to Table II, parameters for the LiPF6 electrolytes were obtained using the 100% extrapolated IR correction method of two measurement series. The activity coefficient was fitted using Eq. 33.

Electrolyte	ε_r [−]	U_{Ref} [V]	$\dot{a}$ [nm]	x_1 [−]	R^2 [−]
$LiClO_4$ in EC:DEC (1:1, w:w)	35 ± 3	3.3079 ± 0.0042	12.8 ± 23.4	0.907 ± 0.005	0.996
$LiPF_6$ in EC:DMC (1:1, w:w)	38 ± 6	3.2941 ± 0.0001	4.5 ± 1.1	1.146 ± 0.012	0.995
$LiPF_6$ in EC:DMC (3:7, w:w)	23 ± 3	3.3030 ± 0.0005	$3.5 \cdot 10^4$	1.207 ± 0.010	0.996
$LiPF_6$ in EC:EMC (3:7, w:w)	22 ± 3	3.3101 ± 0.0003	$4.0 \cdot 10^4$	1.347 ± 0.006	0.998

for the low-concentration region, but also for the high-concentration region, as the obtained activity coefficients have an undefined offset throughout.

While our new methodology cannot provide activity coefficients, we will now show that it does provide accurate values for the so-called thermodynamic factor (TDF). In the equations of the concentrated electrolyte theory, the binary activity coefficient appears in the form of the TDF, defined as

$$\mathrm{TDF} = \left(1 + \frac{\mathrm{d}\ln f_{\pm}}{\mathrm{d}\ln c}\right) = \left(1 + c\frac{\mathrm{d}\ln f_{\pm}}{\mathrm{d}c}\right) \quad [37]$$

The TDFs shown in Figure 9b are based on an exact derivative of Eq. 33, with the parameters from Table III and inserted into Eq. 37. Only in the inset of Figure 9b, for concentrations below 5 mM, the impact of the Debye-Hückel behavior to the TDF can be seen, illustrating its negligible contribution at normal electrolyte concentrations (1 M). Mathematically this can also be shown with the ratio of TDFs based on Eq. 33 with and without the Debye-Hückel term. Using the parameters from Table III for the electrolyte with the largest Debye-Hückel behavior, $LiPF_6$ in EC:DMC (1:1, w:w), a ratio of 98% is found at a concentration of 5 mM.

$$\left[1 + c\cdot\frac{\mathrm{d}}{\mathrm{d}c}\left(-A\sqrt{c}\left(1+Ba\sqrt{c}\right)^{-1} + x_1 c\right)\right] \Big/ \left[1 + c\cdot\frac{\mathrm{d}}{\mathrm{d}c}\left(x_1 c\right)\right] = 0.98 \quad [38]$$

In Eq. 38 the ferrocenium contribution to the ionic strength is neglected, i.e., $I = c$. We conclude, that due to the dependence of the TDF on the derivative of the logarithmic activity coefficient with respect to salt concentration, an exact knowledge of the low-concentration range and of the offset from the Debye-Hückel behavior mentioned above is not required. For most lithium ion battery applications the accuracy of the TDF at concentrations around and below 5 mM is not essential and an accurate value of the TDF between 5 mM and 2 M salt concentrations should be sufficient for most battery models. In this concentration range the TDFs can be well represented (error $< 2\%$ compared to full Debye-Hückel description) by a linear function as demonstrated with Eq. 38.

Our results for the TDFs are summarized in Figure 9b, showing similar trends for all $LiPF_6$ based electrolytes investigated (red colors) and slightly smaller values for the $LiClO_4$ containing electrolyte (blue). While former electrolytes range between a value of 2.15 and 2.35 for the TDF at 1 M salt concentrations, for the latter $LiClO_4$ electrolyte a value of 1.9 is found. A variation of the solvent ratio or replacement of the unpolar component only results in a small change of the TDF of the $LiPF_6$ electrolytes. Further investigations are necessary to quantify the individual salt and solvent contributions to the activity coefficient and the thermodynamic factor in order to give a precise description of the underlying principles.

Comparison with the literature.—A comparison of the TDFs of $LiPF_6$ containing electrolytes investigated by us, with those reported in the literature for similar electrolytes, is shown in Figure 10. All our $LiPF_6$ electrolytes, which were chosen as they represent standard electrolytes for lithium ion batteries, fall in a reasonably narrow range. Thus, they are represented by the red highlighted area in Figure 10, encompassing the red lines in Figure 9b. As the electrolytes investigated in literature are similar to ours, we would expect them to lie in or close to our range. A direct comparison with our data is possible for the electrolyte $LiPF_6$ in EC:EMC, 3:7 w:w, which was also analyzed by Nyman et al.[7] (brown). An excellent agreement is found at concentrations above 1 M; the values for the reported TDF lie within or are very close to our range of TDFs for $LiPF_6$ electrolytes. The deviation between our values and the values reported by Nyman et al.[7] (brown) at salt concentration below 1 M may be a result of the different determination technique used. Nyman et al.[7] determine the TDF, the transference number and the diffusion coefficient at once, based on experiments in a polarization cell and a concentration cell and assume polynomial functions for the parameters. The same procedure is

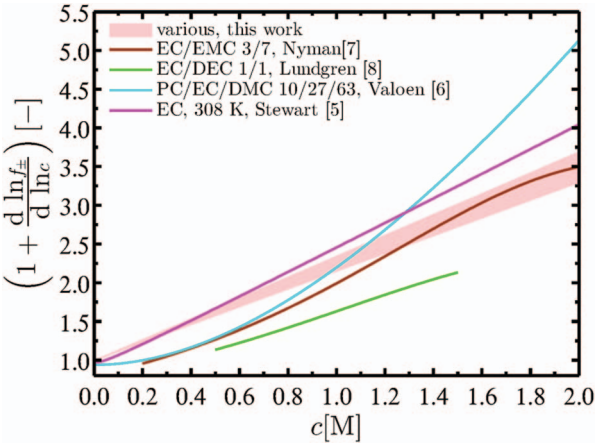

Figure 10. Comparison of determined thermodynamic factor for various $LiPF_6$ containing electrolytes (data from this work marked by red highlighted area) with TDFs published with similar solvents: Nyman:[7] $LiPF_6$ in EC:EMC, 3:7, w:w; Lundgren:[8] $LiPF_6$ in EC:DEC, 1/1, w:w; Valøen:[6] $LiPF_6$ in PC:EC:DMC, 10:27:63, v:v:v; Stewart:[5] $LiPF_6$ in EC:EMC, 1:1, w:w.

used by Lundgren et al.,[8] who also report smaller values for the electrolyte $LiPF_6$ in EC:DEC, (1/1, w:w) containing electrolyte (green) compared to our range. While in latter publications the behavior at low concentrations is neglected, Stewart and Newman[5] (magenta) and Valøen et al.[6] (turquoise) assume a Debye-Hückel behavior. In the publication by Stewart and Newman, a Debye-Hückel behavior as described by Eq. 33 is assumed for small concentrations.[5] In this case, the Debye-Hückel behavior also does not affect the curvature of the resulting TDF, but only imposes a small correction at the lowest concentrations. In the TDF determined by Valøen et al. a distinct, non-linear trend at low concentrations can be observed.[6] Valøen et al. assume the natural logarithm of the mean molar activity coefficient to be a series expansion of $\sqrt{c}$ terms. This formulation does not allow for a fast deviation from the linear Debye-Hückel behavior and thus leads to a pronounced negative feature in the TDF. We want to emphasize that in the literature generally more than one experiment was used to obtain the TDF.

In summary, we find the application of the presented methodology, i.e. determination of the thermodynamic factor based on the slope of the activity coefficient, shows good agreement with literature. We conclude, our analysis of reproducible measurements allows for a precise determination of the thermodynamic factor in a concentration range from 5 mM to 2 M.

Conclusions

In this contribution, we demonstrated the validity of determining the thermodynamic factor based on measurements conducted in a standard three electrode glass cell. Therefore we use cyclic voltammetry and measure the redox potentials of the ferrocene/ferrocenium couple vs. a lithium electrode immersed in electrolytes with variable lithium salt concentrations. The relation between the half-wave potentials and the mean molar activity coefficient of the lithium salt is derived in detail in order to unravel the underlying principles of the measurement and to understand the limits of the experimental methodology due to non-ideal effects caused by deviation from Nernstian redox behavior and from diffusion overpotentials. To evaluate the influence of non-ideal effects, the peak separation between the ferrocene/ferrocenium oxidation and reduction peak potentials is used as a quality measure for the experimental data. It is emphasized that correct ohmic drop compensation has to be performed in order to obtain reliable results. The half-wave potentials vs. lithium salt concentration were successfully correlated with an extended Debye-Hückel law by fitting. Extracted fitting parameters allow to precisely describe the trend of the activity coefficient at salt concentrations above 5 mM, but do not allow quantification of the absolute value of the activity coefficient.

However, the quantity of interest for battery simulations based on the concentrated solution theory, the thermodynamic factor, depends on the slope of the activity coefficient and can thus be calculated precisely by our new method from the parameters obtained by the extended Debye-Hückel fit. For better comparability with literature data, measurements were conducted in a concentration range from 5 mM to 2 M for three $LiPF_6$ containing electrolytes. Comparison of our TDF data with the literature shows the same qualitative, mostly linear trends and for similar electrolytes good agreement is found. The error made by assuming a linear TDF instead of the full description, including the Debye-Hückel behavior, is <2%. Within a ∼5% range, the TDF for the electrolytes $LiPF_6$ in EC:DMC (1:1, w:w), EC:DMC (3:7, w:w) and EC:EMC (3:7, w:w) can be described by $\mathrm{TDF}(c) = 1 + 1.25c$. Accordingly we find $\mathrm{TDF}(c) = 1 + 0.91c$ for the electrolyte $LiClO_4$ in EC:DEC (1:1, w:w). As mentioned in the introduction, also the temperature dependence of the thermodynamic factor should be investigated in detail. While this work provides a thorough description of the experimental setup and the measurement technique, the temperature dependence of the thermodynamic factor will be subject of a future study.[12]

Acknowledgment

We gratefully acknowledge the funding by the Bavarian Ministry of Economic Affairs and Media, Energy, and Technology for its financial support under the auspices of the EEBatt project. Many thanks to Qi He for the coaxial cell setup for measuring the relative permittivities. We thank Ram Subbaraman and Nathan Craig for valuable discussions.

Note added in proof.—The assumption of the redox potential of the Fc/Fc^+ couple not being strongly influenced by the $LiClO_4$ concentration made in the Theory section can also be verified by measurements conducted by Pendley et al., who showed a constant potential of the Fc/Fc^+ couple versus a sodium saturated calomel electrode in different concentrations of supporting electrolyte as long as the concentration ratio of ferrocene to supporting electrolyte is small.[26]

List of Symbols

Symbol	Name	Unit
$\gamma_\pm$	mean molal activity coefficient	-
$f_\pm$	mean molar activity coefficient	-
a_n^θ	prop. constant for the secondary ref. state	L/mol
$(1+\frac{\mathrm{d}\ln f_\pm}{\mathrm{d}\ln c})$	thermodynamic factor	-
U	cell potential	V
ϕ	electrostatic potential wrt. anionic species	V
c	concentration	mol/L
ν_i	stoichiometry factor	-
μ	chemical potential of uncharged species	J/mol
$\tilde{\mu}$	chemical potential of ionic species	J/mol
$\Delta_R G$	reaction Gibbs energy	J/mol
z_i	ionic charge (neg./pos. for anions/cations)	-
μ^θ	standard chemical potential	J/mol
μ_{Cell}	standard chemical cell potential	J/mol
U_0'	formal potential of WE wrt. RE	V
s	scan rate in cyclic voltammogram (CV)	mV/s
t	time	s
$U_{\mathrm{p.ox/red}}$	oxidation / reduction peak potential	V
$I_{\mathrm{p.ox/red}}$	oxidation / reduction peak current	A
D_i	diffusion coefficient of species i	cm^2/s
U_{reverse}	cyclic voltammogram (CV) vertex potential	V
η	kinetic overpotential	V
Ψ	dimensionless parameter relating CV peak separation with the rate constant	-
α	transfer coefficient in Butler Volmer eqn.	-
k_0	standard rate constant	1/s
$U_{\mathrm{p.1/2}}$	cyclic voltammogram half-wave potential	V
i	current density	A/cm^2
κ	electrolyte conductivity	mS/cm
t_i	transference number of ionic species i	-
R	resistance	Ω
I	ionic strength	mol/L
$\dot{a}$	distance of closest approach	nm
ε_R	relative permittivity of electrolyte	-

Constants

F	Faraday constant	C/mole
R	gas constant	J/(mole K)
T	temperature	K
ε_0	vacuum permittivity	F/m
N_A	Avogadro constant	-
k	Boltzmann constant	J/K

References

1. J. Newman and K. Thomas-Alyea, *Electrochemical Systems*, 3rd ed., Wiley Interscience, Hoboken, (2004).
2. A. Latz and J. Zausch, *J. Power Sources*, **196**, 3296 (2011).
3. J. Barthel, R. Neueder, H. Poepke, and H. Wittmann, *J. Solution Chem.*, **27**, 1055 (1998).
4. J. Barthel, R. Neueder, H. Poepke, and H. Wittmann, *J. Solution Chem.*, **28**, 489 (1999).
5. S. Stewart and J. Newman, *J. Electrochem. Soc.*, **155**, A458 (2008).
6. L. O. Valøen and J. N. Reimers, *J. Electrochem. Soc.*, **152**, A882 (2005).
7. A. Nyman, M. Behm, and G. Lindbergh, *Electrochim. Acta*, **53**, 6356 (2008).
8. H. Lundgren, M. Behm, and G. Lindbergh, *J. Electrochem. Soc.*, **162**, 3 (2014).
9. H. S. Harned and D. M. French, *Ann. N. Y. Acad. Sci.*, **46**, 267 (1945).
10. Y. Ma, M. Doyle, T. F. Fuller, M. M. Doeff, L. C. Jonghe, and J. Newman, *J. Electrochem. Soc.*, **142**, 1859 (1995).
11. G. Gritzner and J. Kuta, *Pure Appl. Chem.*, **54** (1982).
12. J. Landesfeind, A. Ehrl, M. Frankenberger, W. A. Wall, and H. A. Gasteiger, *J. Electrochem. Soc.*, To be submitted.
13. C. Daniel and J. O. Besenhard, *Handbook of Battery Materials*, Wiley-VCH, (2011).
14. A. Bard and L. Faulkner, *Fundamentals and applications*, 2nd ed., John Wiley & Sons, Ltd, New York, (2004).
15. G. Gritzner, K. Danksagmüller, and V. Gutmann, *J. Electroanal. Chem.*, **72**, 177 (1976).
16. C. H. Hamann, A. Hamnett, and W. Vielstich, *Electrochemistry*, Wiley-VCH, Weinheim, (2007).
17. M. R. Wright, *An Introduction to Aqueous Electrolyte Solutions*, John Wiley & Sons, Ltd, Chichester, (2007).
18. A. M. Bond, K. B. Oldham, and G. A. Snook, *Anal. Chem.*, **72**, 3492 (2000).
19. W. Schmickler and E. Santos, *Interfacial electrochemistry*, Oxford University Press, New York, (1996).
20. H. Scholl and K. Sochaj, *Electrochim. Acta*, **36**, 689 (1991).
21. Y. Wang, E. I. Rogers, and R. G. Compton, *J. Electroanal. Chem.*, **648**, 15 (2010).
22. I. Ruff, V. J. Friedrich, K. Demeter, and K. Csillag, *J. Phys. Chem.*, **75**, 3303 (1971).
23. L. M. Peter, W. Dürr, P. Bindra, and H. Gerischer, *J. Electroanal. Chem.*, **71**, 31 (1976).
24. J. Redepenning, E. Castro-Narro, G. Venkataraman, and E. Mechalke, *J. Electroanal. Chem.*, **498**, 192 (2001).
25. M. S. Ding, *J. Electrochem. Soc.*, **150**, A455 (2003).
26. B. D. Pendley, H. D. Abruna, J. D. Norton, W. E. Benson, and H. S. White, *Anal. Chem.*, **63**, 2766 (1991).